J. Fluid Mech. (1988), *vol.* 187, *pp.* 435–449
Printed in Great Britain

Stability bounds on turbulent Poiseuille flow

By G. R. IERLEY
Fluids Research Oriented Group, Department of Mathematical Sciences,
Michigan Technological University, Houghton, MI 49931, USA

AND W. V. R. MALKUS
Department of Mathematics, Massachusetts Institute of Technology,
Cambridge, MA 02139, USA

(Received 24 March 1986 and in revised form 24 August 1987)

For steady-state turbulent flows with unique mean properties, we determine a sense in which the mean velocity is linearly supercritical. The shear-turbulence literature on this point is ambiguous. As an example, we reassess the stability of mean profiles in turbulent Poiseuille flow. The Reynolds & Tiederman (1967) numerical study is used as a starting point. They had constructed a class of one-dimensional flows which included, within experimental error, the observed profile. Their numerical solutions of the resulting Orr-Sommerfeld problems led them to conclude that the Reynolds number for neutral infinitesimal disturbances was twenty-five times the Reynolds number characterizing the observed mean flow. They found also that the first nonlinear corrections were stabilizing. In the realized flow, this latter conclusion appears incompatible with the former. Hence, we have sought a more complete set of velocity profiles which could exhibit linear instability, retaining the requirement that the observed velocity profile is included in the set. We have added two dynamically generated modifications of the mean. The first addition is a fluctuation in the curvature of the mean flow generated by a Reynolds stress whose form is determined by the neutrally stable Orr–Sommerfeld solution. We find that this can reduce the stability of the observed flow by as much as a factor of two. The second addition is the zero-average downstream wave associated with the above Reynolds stress. The three-dimensional linear instability of this modification can even render the observed flow unstable. Those wave amplitudes that just barely will ensure instability of the observed flow are determined. The relation of these particular amplitudes to the limiting conditions admitted by an absolute stability criterion for disturbances on the mean flow is found. These quantitative results from stability theory lie in the observationally determined Reynolds–Tiederman similarity scheme, and hence are insensitive to changes in Reynolds number.

1. Introduction

This study is an exploration of various mechanisms that affect the stability of statistical quantities in steady-state turbulent flow. An ultimate goal of such inquiry is to isolate the principal physical processes that determine the equilibration of the flow.

Here we examine the traditional inhomogeneous steady-state problem of Poiseuille flow in channels. The geometry of the coordinate system to describe this flow is given

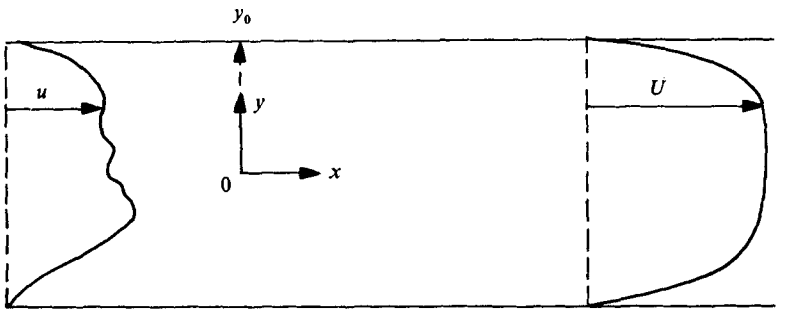

FIGURE 1. The configuration for turbulent Poiseuille flow considered in this paper.

in figure 1. The velocity of the fluid, $\boldsymbol{v}$ is divided into a mean and fluctuating part:

$$\boldsymbol{v} = \boldsymbol{U}+\boldsymbol{u}, \quad \boldsymbol{U} = \bar{\boldsymbol{v}}, \quad \overline{(\ )} = \lim_{t\to\infty}\frac{1}{T}\int^{T}(\ )\,\mathrm{d}t \tag{1.1}$$

The mean part is indicated by an overbar, and the overbar is taken in this context to be a local time-average of the flow. The time-averaged Navier–Stokes equation for the incompressible fluid being studied is written

$$\boldsymbol{U}\cdot\nabla\boldsymbol{U}+\overline{\boldsymbol{u}\cdot\nabla\boldsymbol{u}}+\frac{\nabla\bar{P}}{\rho}-\nu\nabla^2\boldsymbol{U} = 0, \tag{1.2}$$

while the corresponding equation for the fluctuating velocity $\boldsymbol{u}$ is

$$\frac{\partial\boldsymbol{u}}{\partial\tau}+\boldsymbol{u}\cdot\nabla\boldsymbol{U}+\boldsymbol{U}\cdot\nabla\boldsymbol{u}+\frac{\nabla P}{\rho}-\nu\nabla^2\boldsymbol{u} = (\overline{\boldsymbol{u}\cdot\nabla\boldsymbol{u}}-\boldsymbol{u}\cdot\nabla\boldsymbol{u}). \tag{1.3}$$

The fluctuation–fluctuation interaction terms on the right-hand side of (1.3) play a disputed role in the overall energetics of the fluctuating field.

In simplistic theories of turbulence these right-hand terms are treated as the source of 'eddy viscosity'. In more ornate statistical theories (e.g. Lagrangian History Direct Interaction Approximation, Kraichnan 1962), they act as stabilizing radiators of energy into wavenumber space. These terms have also been shown to be stabilizing in convection mean-field theories (Herring 1963, 1964; Claussen 1983), and upper-bound theories (Chan 1971). However, we also know that such terms can be destabilizing, at least in transient subcritical bifurcation of one-dimensional $\boldsymbol{U}$-fields (Herbert 1980; Orszag & Patera 1981). If these fluctuation–fluctuation terms prove to be stabilizing, then the observed $\boldsymbol{U}$-fields must be linearly unstable. We shall explore here how stable or unstable such fields actually are.

2. Statistical stability

For a function $\boldsymbol{U}(y)$ to represent the mean of a turbulent flow, isolated disturbances from that mean must eventually decay. This is a first sense in which the field $\boldsymbol{U}$ is stable. Also, observations indicate that $\boldsymbol{U}$ is a continuously changing function of the Reynolds number. Hence, beyond the laminar range the entire function $\boldsymbol{U}(y, R)$ is marginally stable. Tractable stability problems to determine the $\boldsymbol{U} = \boldsymbol{U}(y, R)$ realized in experiment have been found for small-amplitude unstable flows which are

steady or periodic. However, previous stability studies for non-periodic flows rest on *ad hoc* assumptions.

One possibility that can provide a quantitative indication of stable $\boldsymbol{U}$-fields is the use of the dissipation-rate integral. Derived by multiplying (1.3) by $\boldsymbol{u}\cdot$ and averaging over the whole domain, it is

$$\frac{\partial}{\partial\tau}\langle\tfrac{1}{2}\boldsymbol{u}\cdot\boldsymbol{u}\rangle+\langle\boldsymbol{u}\cdot\boldsymbol{u}\cdot\nabla\boldsymbol{U}\rangle-\nu\langle\boldsymbol{u}\cdot\nabla^2\boldsymbol{u}\rangle=0. \tag{2.1}$$

This integral has lost the advective nonlinearity of the Orr–Sommerfeld-like operator of (1.3) and retains only the shear terms as the direct energy source for potential disturbances. Treated as a variational statement of an eigenvalue problem, it is known to give considerably lower bounds on the Reynolds number than is characteristic of laminar shear flow (Joseph 1976). It is also established that, treated as an integral constraint to determine upper bounds on momentum transfer (Busse 1978), it gives bounds considerably in excess of those observed in turbulent flow. The reasons are rather clear. These problems have lost the essential constraint of travelling-wave solutions which are characteristic of (1.3).

3. Stability boundaries for the mean-field disturbance equation

In the spirit of an earlier paper by Reynolds & Tiederman (1967), here we plan a numerical exploration of the stability of a large class of functions treated as possible mean profiles $\boldsymbol{U}(y)$ and containing in the class a member indistinguishable from the observed profile. The Reynolds–Tiederman empirical two-parameter family of functions is augmented here by the infinite set of waves which are eigensolutions of the stability problems.

The two-parameter family of functions chosen by Reynolds & Tiederman reflects much accumulated observational and theoretical experience on appropriate scaling for turbulent flows. A central part of this study is to determine how that presumed scaling is related to the stability properties. They chose to study the functions

$$U(y)=RB\int_0^y\frac{1-y'}{1+E(y')}\,\mathrm{d}y', \tag{3.1}$$

where

$$R=\frac{\langle U\rangle y_0}{\nu},\quad B=-\frac{\partial P}{\partial x}(y=0),\quad \int_0^1 U\,\mathrm{d}y=1, \tag{3.2}$$

and

$$E(y)=\frac{1}{2}\left\{1+\frac{K^2R^2B}{9}(2y-y^2)^2(3-4y+2y^2)^2\left(1-\exp\frac{-yRB^{\frac{1}{2}}}{A}\right)^2\right\}^{\frac{1}{2}}-\tfrac{1}{2}. \tag{3.3}$$

The (Van Driest) boundary-layer-like quantity A and the von Kármán-like quantity K were the two parameters considered by Reynolds & Tiederman. They show that the choice $A=31$, $K=0.4$, leads to profiles within the experimental error of all observations made by J. Laufer, The quantity $RB^{\frac{1}{2}}$ is the friction Reynolds number, and appears in $E(y)$ to reflect the observed scaling as the Reynolds number R becomes large. Here we shall test the preservation of this scaling as Reynolds stresses due to finite-amplitude waves alter the effective $E(y)$.

The linear stability problem for $U(y,R)$, from (1.3) and (3.1), is written

$$\psi^{\mathrm{IV}}-2\alpha^2\psi''+\alpha^4\psi=\mathrm{i}\alpha R^*[(U(y,R)-c)(\psi''-\alpha^2\psi)-U''(y,R)\psi]. \tag{3.4}$$

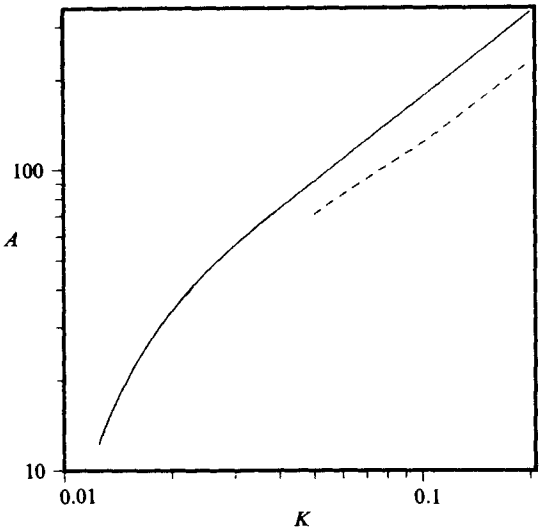

FIGURE 2. The neutral stability curve for the Orr–Sommerfeld equation using a family of profiles parametrized by the (A, K)-plane. The original results of Reynolds & Tiederman (1967) are illustrated by the dashed line.

Reynolds & Tiederman sought the eigensolution ψ and values for α which led to a minimum R^* for many members of the set $U(y, R)$. Their purpose was to discover the particular values of A and K for which R^*, the critical Reynolds number for instability, was equal to R, the profile Reynolds number. Their quantitative results were achieved by an ingenious mixture of analytic and numerical methods.

We started our exploration by repeating the Reynolds–Tiederman linear stability study using a spectral method of high accuracy as implemented for laminar Poiseuille channel flow by Orszag (1971). The results of this effort are summarized in figure 2.

Figure 2 is a curve in the (A, K)-plane, at a profile Reynolds number of 25000, of those (A, K)-values that led to an $R^* = 25000$. To the right of the curve all (A, K)-pairs are found to represent profiles stable to linear disturbances ($R^* > 25000$), while all (A, K)-pairs to the left of the curve are unstable ($R^* < 25000$). Reynolds & Tiederman's earlier curve is indicated as a dashed line. They concluded, as must we, that the linear stability of the (A, K)-profiles does not determine the quantitative structure of turbulent channel flow, for the curve of marginal stability passes at a considerable distance from the observed (A, K). In addition, they suggested that the disturbances were supercritical where they were unstable.

It is also clear from figure 2 that no unique (A, K) is selected by the linear marginal stability process. It is not clear from figure 2 alone if the marginal curve is the same curve at other Reynolds numbers, that is, whether the linear stability process has the presumed scaling.

The unresolved problems of scaling, profile selection, and the super- or sub-criticality of two- and three-dimensional disturbances are addressed in the following sections. Scaling studies require a considerable number of additional linear solutions at many profile Reynolds numbers. This task is simplified by properties of the Reynolds–Tiederman profile deduced in the next section.

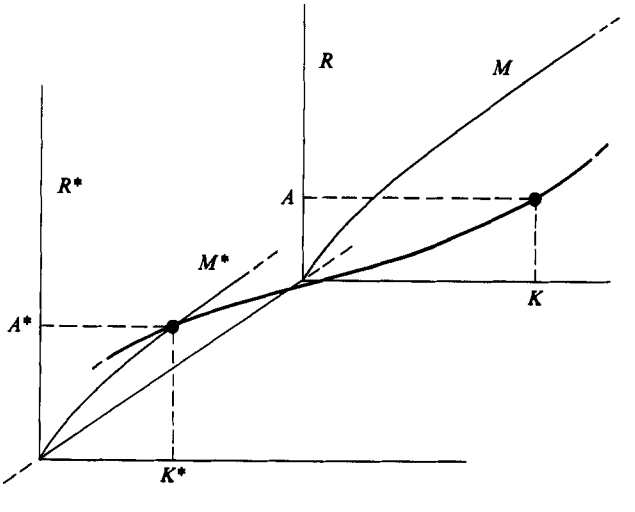

FIGURE. 3. Projection of (A,K)-pairs from the R- to the R^*-plane.

4. Asymptotic scaling

It is seen from (3.1), (3.2) and (3.3) that the profile $U(y)$ depends on R, B, K, A in such a way that if

$$\eta = \frac{A}{RB^{\frac{1}{2}}}, \quad \beta = KRB^{\frac{1}{2}} \tag{4.1}$$

are held fixed, the shape of $U(y)$ is unaltered, and its normalization is preserved if

$$\gamma = RB \tag{4.2}$$

is held fixed. These three constraints among four variables show that U is invariant with respect to the following transformation:

$$\left.\begin{aligned} R &\to R^*, \\ B &\to B^* = B\left(\frac{R}{R^*}\right), \\ A &\to A^* = A\left(\frac{R^*}{R}\right)^{\frac{1}{2}}, \\ K &\to K^* = K\left(\frac{R}{R^*}\right)^{\frac{1}{2}}. \end{aligned}\right\} \tag{4.3}$$

Each profile represented by a point (A,K) in the R-plane has associated with it a minimum marginal eigenvalue, R^* (and an eigensolution ψ, a separation wavenumber α, and a phase velocity c). This profile is transformed by (4.3) to a profile marginally stable in the R^*-plane, i.e. the profile Reynolds number matches the minimum Reynolds number for marginal stability. Figure 3 indicates this relationship in a three-dimensional plot of (A,K) and R. The line of points defined by many (A^*,K^*) pairs on the R^*-plane is the curve of marginal stability M^*, If the linear stability process is related to the observed turbulent phenomena one would expect that the curve of marginal stability, M on the R-plane, asymptotically attains the shape of the curve M^* as both R and R^* become large. Equation (4.3) will help us to answer this question by permitting stability computations made on one R-plane

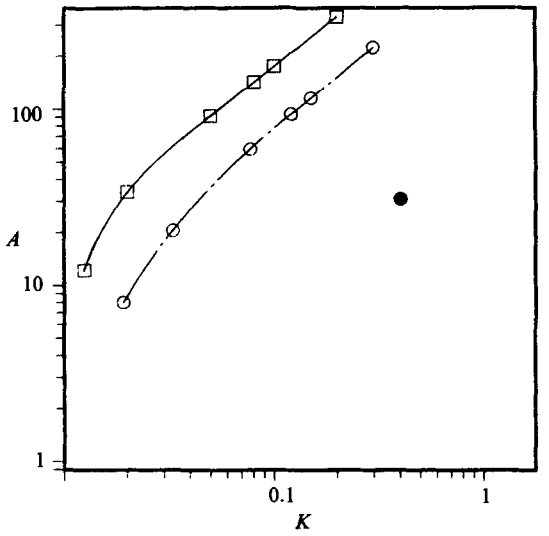

FIGURE 4. Shift in the neutral stability curve due to the addition of the Reynolds stress due to an Orr–Sommerfeld wave: solid line from the original (unmodified) profile; chain dot line from the mean flow plus the Reynolds stress. The black dot is the best fit to laboratory data.

to be projected onto another. However, it is convenient to delay the report on the degree of R-dependence of the stability results until the finite-amplitude and three-dimensional stability problems are addressed.

5. Finite-amplitude instability along the marginal curve

Figure 2 exhibits the curve in the (A, K)-plane that is marginally stable. However we find that the finite-amplitude behaviour of departures from that curve are subcritical, leading to an equilibration at a small finite amplitude very close to the plotted (A, K)-curve. For example, a point in the middle of the curve would be reduced from marginally stable on the $R = 25000$ plane to the $R = 24000$ plane. We believe this small-finite-amplitude behaviour is due to the inability of the (A, K)-plane to reflect the subtle structure of equilibrium profiles attained by the real flow. It is found, then, that the correction is very small except for the existence of a finite-amplitude wave associated with the marginally stable curve.

The next step was to explore the modifications of the marginal curve as a consequence of finite distortion of the mean field due to the Reynolds stress of a wave whose structure was determined by the eigenvalue problem. Lengthy computation indicates that this effect is significant, but also not very large. The principal results of that study are contained in figure 4. There one can see that addition of the Reynolds stress produced by an Orr–Sommerfeld wave to the mean profile leads to a reduction in the critical Reynolds number R^* to below the value it would have in the absence of such a modification. The curve drawn corresponds to a marginal inflexion in the flow and leads to a reduction of R^* of about one-half of its original value. By inviscid theory, such a state lies on the border of instability. However, the magnitude of the local u, v wave velocities required to sustain an inflexion in the mean is uncomfortably large. The large dark point is the observed value of (A, K).

Figure 5 plots the original and modified curvature for $K^* = 0.08$ and $A^* = 142.02$. Figure 6 is a plot of the velocity deduced from the inflected curve and from the

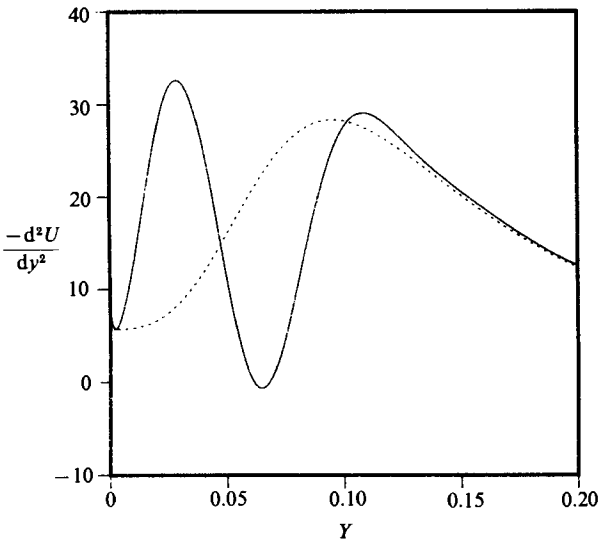

FIGURE 5. Curvature of the original velocity profile (single peak) and modified velocity profile (double peak) due to the addition of the derivative of the Reynolds stress from a neutrally stable Orr–Sommerfeld solution.

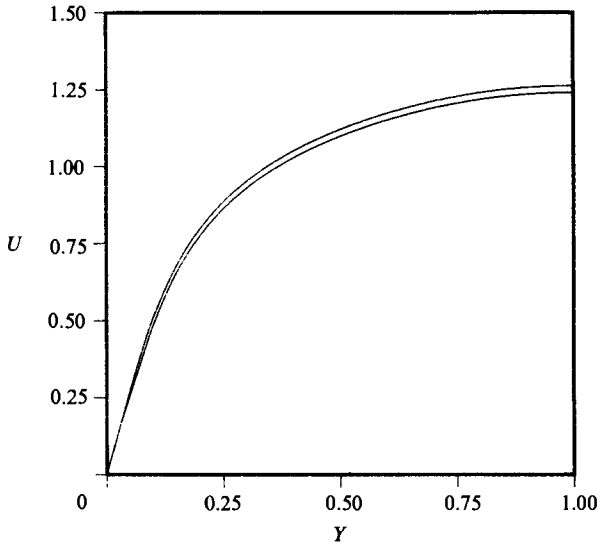

FIGURE 6. The original velocity profile (upper curve) and modified velocity profile (lower curve) due to the addition of the Reynolds stress from a neutrally stable Orr–Sommerfeld solution.

original curve indicating the very small change in the resultant structure. Actually the curve must be renormalized, since the integrated velocity in this representation is one. Having done that, the two curves would be essentially indistinguishable.

We conclude then that, for wave amplitudes that are as large as one could reasonably expect on the mean field, the reduction in the critical Reynolds numbers still does not bring the marginal curve particularly near the observed point on the (A, K)-plane.

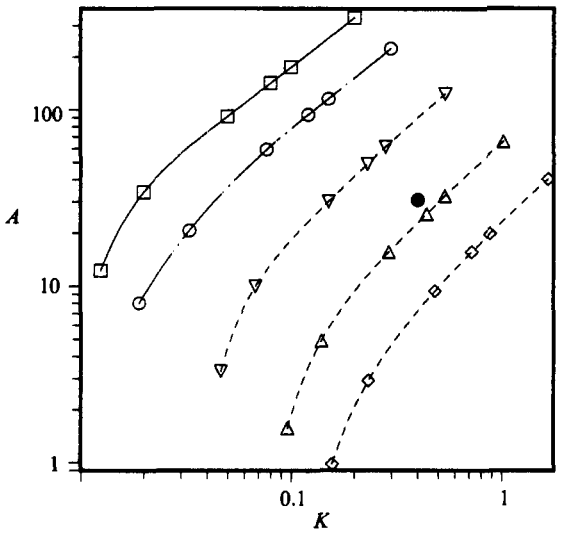

FIGURE 7. Curves of marginal stability for a three-dimensional disturbance on a profile with a finite-amplitude two-dimensional wave field. From left to right the dashed curves represent neutral stability curves for maximal downstream velocities due to the wave of 5, 25 and 100% of the local mean velocity.

6. Three-dimensional instability of the two-dimensional wave

In the previous section we explored the effect on stability of the modification of the mean field only. Recent work by Orszag & Patera suggests the importance of the inertial instability of the two-dimensional wave associated with a finite-amplitude Orr–Sommerfeld solution. They established that three-dimensional instabilities were supercritical at the point of marginality and had inertial growth rates. In that study, the two-dimensional waves were presumed to be imposed on the flow by, perhaps, a vibrating ribbon or some other mechanism, or were an existing post-critical wave after bifurcation of the flow. Here a similar view can be taken, and the destabilizing effect of these waves of finite amplitude will be explored over the entire stable side of the (A,K)-plane. We shall seek a value of wave amplitude appropriate to marginal three-dimensional instability in the entire region to the right of the marginal curve for the mean field. It is not clear that this is possible. There may be a saturation as far as the three-dimensional instability is concerned. In fact such a saturation was suggested by the work of Orszag & Patera. In particular it may be that the amplitudes required are totally unreasonable. Very shortly we shall assess absolute stability, in which the reasonableness of a presumed amplitude can be determined. In our first explorations of this problem, we were deterred by the estimates of machine time needed for a reasonable search of the (A,K)-plane. However, a reduced form of a three-dimensional algorithm due to Zaff (1987), generated in a study of narrow-gap Ekman flow, made use of an IBM 4381-Q02 feasible for determination of critical R^* values for three-dimensional instability.

Figure 7 indicates the curves of marginal three-dimensional instability for three different two-dimensional wave amplitudes. The curve to the right is for a maximum downstream velocity due to the wave that is equal to the local mean velocity. For such a wave, the mean profile at the observed (A,K)-point is quite unstable. The curve that passes nearly through the observed (A,K) is for a wave amplitude leading

to a maximum downstream velocity due to the wave of 25% of the local mean velocity. The curve closest to the original marginal stability curve represents a velocity of 5%. These amplitudes are all a small fraction of that needed to produce a marginal inflexion in the mean. The 100% amplitude corresponds to a total wave energy approximately 1% of the energy in the mean flow.

Also observed was an unusual feature of the eigenvalue spectrum of three-dimensional modes in the vicinity of the observed point $A = 30$, $K = 0.4$ in the $R = 5000$ plane. It would appear that at this point, as many as 15 other vertical modes in eigenstructure are nearly neutrally stable at the same time that the principal vertical mode becomes unstable. This may relate to selection mechanisms which we plan to explore in the near future.

7. Absolute stability

So far we have had no way of judging what amplitudes are permitted the real flow. It has been possible to choose appropriate two-dimensional wave amplitudes to assure mean flows unstable with respect to three-dimensional disturbances since the fluctuation field has been energetically unconstrained. In this section we address the problem of the absolute stability of disturbances of the scale of those generated by the instabilities. The goal is to rule out a range of (A,K)-space as energetically inaccessible to even the most determined three-dimensional disturbance.

At first sight, constraining amplitude by use of absolute stability theory will appear paradoxical since it is a linear theory. Therefore, we begin with a review of the conventional treatment of absolute stability, and next describe a more relevant constrained absolute stability problem. Finally we present the results of an approximate solution to this constrained problem.

The usual approach to the determination of a rigorous lower stability bound on shearing flows, e.g. Joseph (1976), is based on the single dissipation-rate integral (2.1), the continuity condition, and the boundary conditions. The perturbation fields are only weakly constrained by that fraction of the full dynamics that is captured in the moment integral, and a lower bound for stability obtains from the variational problem

$$R_{\text{abs}} = \min_{\boldsymbol{u}} \frac{\langle \boldsymbol{u}\cdot\nabla^2\boldsymbol{u}+\boldsymbol{u}\cdot\nabla\lambda_1\rangle}{\langle \boldsymbol{u}\cdot\boldsymbol{u}\cdot\nabla\boldsymbol{U}\rangle}, \tag{7.1}$$

where λ_1 is a Lagrange multiplier (essentially the pressure field) chosen to enforce incompressibility.

For laminar Poiseuille channel flow, Busse (1969) and Joseph & Carmi (1969) have shown that the minimum eigenvalue attains for a two-dimensional eigensolution which is independent of the downstream coordinate. The Euler–Lagrange equations then follow directly as

$$\left.\begin{aligned} 2\left(\frac{\mathrm{d}^2}{\mathrm{d}y^2}-\alpha^2\right)^2 v(y)-\alpha^2 R\frac{\mathrm{d}\bar{U}}{\mathrm{d}y}u(y)=0,\\ 2\left(\frac{\mathrm{d}^2}{\mathrm{d}y^2}-\alpha^2\right)u(y)+R\frac{\mathrm{d}\bar{U}}{\mathrm{d}y}v(y)=0,\end{aligned}\right\} \tag{7.2}$$

where $v(\pm 1) = v'(\pm 1) = u(\pm 1) = 0$. (This system is easily solved as a two-component generalized eigenvalue system using a Chebyshev series expansion of the

eigenfunctions. Newton's method to optimize the cross-stream wavenumber converges rapidly for nearly any initial estimate. Two tests on accuracy are available, plane Couette flow, and channel Poiseuille flow. Couette flow leads to an eigenvalue problem identical with that of thermal Boussinesq convection with rigid boundary conditions. Rescaling values of (α, R) to compensate for a unit half-channel width in the shear-flow case, we reproduce the values for convection theory of (3.1167, 1707.7545). Our result for laminar Poiseuille flow is (2.0442, 49.6035), corroborating the value found by Busse.)

In turbulent Poiseuille flow the mean profile is dynamically sustained by Reynolds stresses due to any scales of motion. The smallest scale, determining the boundary region, is the most demanding energetically (Malkus 1956). It is the absolute stability of this scale we wish to establish. It is not evident whether this smallest scale is associated with two- or three-dimensional disturbances, but we find for the eigenstructures reported on earlier in the paper that the three-dimensional Reynolds stresses have a larger cross-stream scale than those produced by the two-dimensional wave field. Hence, we explore the absolute stability of the Orr–Sommerfeld wave scale which differs for each pair of values in the (A, K)-plane.

From the linear theory we determine the form of the local mean Orr–Sommerfeld Reynolds stress, $\overline{u'v'}(A, K, y)$, for a particular (A, K)-profile. We then require that the solution of the *absolute* stability problem have a Reynolds stress of identical form and impose this with an added Lagrange multiplier in the variational statement. Specifically, we seek the R satisfying

$$R_{\text{abs}} = \min_{\boldsymbol{u}} \frac{\langle \boldsymbol{u} \cdot \nabla^2 \boldsymbol{u} + \boldsymbol{u} \cdot \nabla \lambda_1 + \lambda_2(y)(\overline{uv} - \overline{u'v'}) \rangle}{\langle \boldsymbol{u} \cdot \boldsymbol{u} \cdot \nabla \boldsymbol{U} \rangle}. \tag{7.3}$$

The eigenvalue we obtain will equal the profile Reynolds number along some curve in the (A, K)-plane. In contrast to the linear marginal curve far to the left of the observed (A, K), figure 2, this curve must lie to the right of the observed (A, K)-point, for, of course, the observed point is permitted energetically. However, it could turn out to be an even poorer bound of the realized instability than one finds in the laminar case.

The Euler–Lagrange equations derived from (7.3) are a simple and interesting generalization of (7.2):

$$\left.\begin{aligned} 2\left(\frac{\mathrm{d}^2}{\mathrm{d}y^2} - \alpha^2\right)^2 v(y) - \alpha^2 \left[R\frac{\mathrm{d}\bar{U}}{\mathrm{d}y} - \lambda_2(y)\right] u(y)\, 0, \\ 2\left(\frac{\mathrm{d}^2}{\mathrm{d}y^2} - \alpha^2\right) u(y) + \left[R\frac{\mathrm{d}\bar{U}}{\mathrm{d}y} - \lambda_2(y)\right] v(y) = 0, \\ u(y)\, v(y) = \overline{u'v'}_{\text{OS}}, \end{aligned}\right\} \tag{7.4}$$

where $v(\pm 1) = v'(\pm 1) = u(\pm 1) = 0$. This problem appears to be novel in form, and we are unaware of any standard solution strategies. It requires the determination of an unknown coefficient function, $\lambda_2(y)$, which will generate a (u, v)-pair satisfying a quadratic constraint.†

† It has a partial analogue in dynamo theory where a (u, v)-pair of two-dimensional fields are required to satisfy a quadratic integral constraint known as the Taylor constraint (Malkus & Proctor 1975). Only a few special solutions are known.

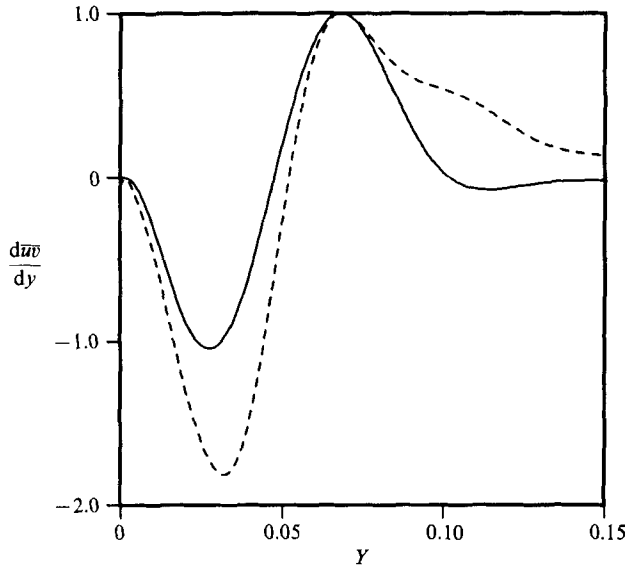

FIGURE 8. A comparison of the derivative of the Reynolds stress from solutions of the Orr–Sommerfeld equation (solid curve) with that from the constrained absolute stability problem (dashed curve). A first match of smallest scales has been produced by truncating the mean shear.

As a first step in the determination of R_{abs} we have adopted an approximate approach. Equation (7.4) depends only on the shear in the mean profile, and not, as in the Orr–Sommerfeld problem, the curvature. The structure of (7.4) suggests a boundary-layer formulation. We reflect this aspect of the absolute stability problem by selecting a first λ_2 as follows:

$$\lambda_2(y) = 0 \qquad (1 > |y| > y_c)$$

$$= R\frac{d\bar{U}}{dy} \quad (y_c \geqslant |y| \geqslant 0).$$

We choose y_c so as to satisfy the third equation in (7.4) as well as possible. In practice, matching the derivative of the Reynolds stress is a more sensitive test, hence we have chosen y_c so that the location of the maximum in the Reynolds stress derivative due to the optimal solution of the dissipation-rate integrals matches that of the Orr–Sommerfeld solution. We find y_c is typically 90% of the distance to the peak in Reynolds-stress derivative determined from the Orr–Sommerfeld solution. Figure 8 exhibits such a match (the dashed curve is from the absolute stability solution). One knows for standard variational problems that the eigenvalues are correct to second order if the eigenfunctions are first-order accurate. It is not evident that this holds when the constraint is only approximately satisfied, nonetheless, initial explorations suggest that the exact eigensolution and eigenvalue of (7.4) will not differ qualitatively from the results reported here.

The marginal curve of constrained absolute stability obtained in this first approximation is drawn on figure 9, as is the original linear marginal curve. It is far from that curve, as anticipated, and includes the observed (A, K) to its left as energetically possible. However this curve *is* remarkably close to the observed (A, K) and corresponds to a local downstream fluctuation velocity no larger than

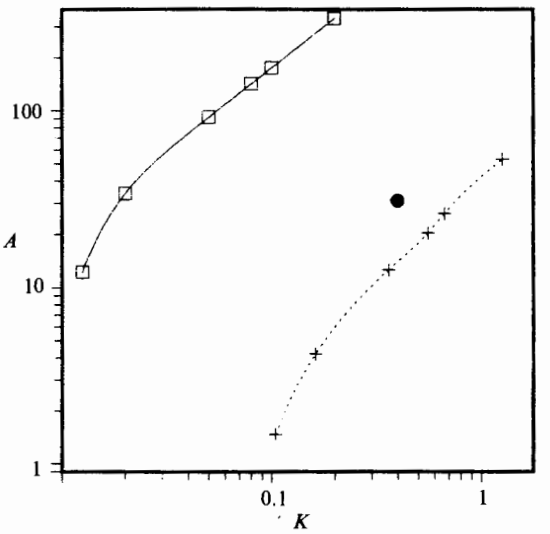

FIGURE 9. The curve of marginal stability for the constrained absolute stability problem discussed in §7. Points to the left of the dotted line are energetically allowed and hence include the observed flow.

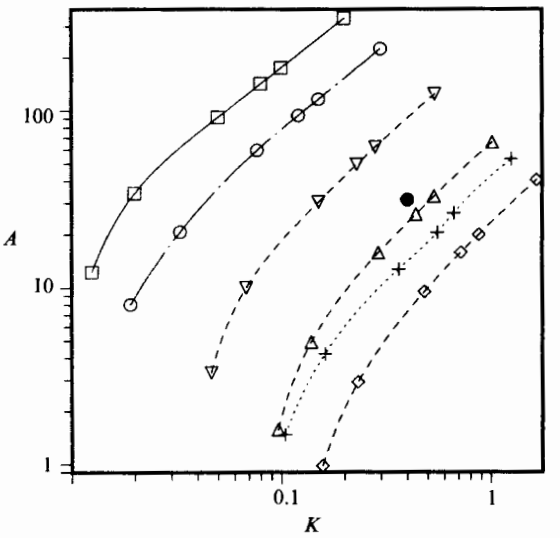

FIGURE 10. A superposition of all the stability results obtained in this paper. The original stability curve (solid line), the two-dimensional reduction (chain dot line), the three-dimensional reductions (dashed lines), and the bound provided by the constrained absolute stability results (dotted line).

approximately 40% of the local mean value. It is encouraging that such a bound is close to the observations, and suggests that the three-dimensional instabilities of shear turbulence significantly relax the constraints on the release of shear energy inherent in the linear theory.

In figure 10 the entire family of stability results are combined. The linear marginally stable curve, the absolute marginally stable curve, and the three-dimensional marginally stable curves for maximum wave amplitudes of 5%, 25%, and 100%, are all drawn on the same graph.

8. Insensitivity to changes in Reynolds number

To some readers it may be surprising that the results established for this particular $R = 25000$ plane obtain more generally. Perhaps most unanticipated is that scaling of *both* the three-dimensional and the constrained absolute instabilities persists on this plane. This implies that the equilibrating process is intimately and intricately linked to the two- and three-dimensional instability mechanisms we explore here.

This scaling is established using a formulation of (3.3) to project from other planes onto this 25000 plane. The errors are less than 10% even for original points on the marginal curve corresponding to Reynolds numbers of a few thousand. To illustrate this we sketch the process of scaling for a few representative points. For clarity, we recall here the scaling results from (4.3):

$$\frac{A^*}{A} = \left(\frac{R^*}{R}\right)^{\frac{1}{2}}, \quad \frac{K^*}{K} = \left(\frac{R}{R^*}\right)^{\frac{1}{2}}.$$

For two-dimensional disturbances we take as an example the point $K = 0.12$, $A = 95$, which for a profile Reynolds number R of 25000 is neutrally stable at $\alpha = 3.8$ and $R^* = 50500$ (where R^* is the coefficient in the Orr–Sommerfeld equation). Equation (4.3) is used to refer this (A, K)-pair to a profile of identical shape function, but with $R = 50500$. We obtain $K = 0.084$, $A = 135$. The marginal stability curve passes through this coordinate pair and lies in the $R = R^* = 50500$ plane. It can be compared with the independent result $K = 0.080$, $A = 142$ found for the $R = R^* = 25000$ plane. We see a shift by about 5% towards the observational data by doubling the Reynolds number. It is possible that this curve simply continues to creep ever closer to the observed data, but we suggest a 5% change for a 2:1 variation in R is evidence for the existence of an asymptotic limit that does not differ qualitatively from the results given here for $R = 25000$.

For three-dimensional disturbances, we consider the point $K = 0.12$, $A = 95$, and $R = 25000$, which is neutrally stable at $R^* = 1720$ for $\beta = 2.65$ when a two-dimensional wave field is used whose maximum local downstream velocity is 25% of the local mean. As a projected (A, K)-pair in the $R = R^* = 1720$ plane, this yields (0.46, 24.8). If we begin with $K = 0.08$, $A = 142$, and $R = 25000$, the corresponding three-dimensional instability result maps onto (0.40, 28.6) in the $R = R^* = 825$ plane. This shift of about 15% in the direction of greater stability suggests that asymptotic two-dimensional wave amplitudes of less than 25% are adequate for three-dimensional marginal stability.

For the constrained absolute stability problem, projections of the same initial (A, K)-pair give $K = 0.59$, $A = 19.2$ for $R = R^* = 1030$, and $K = 0.57$, $A = 20.0$ for $R = R^* = 495$, a shift of only 4% away from the observed point. Interestingly enough, laminar plane Poiseuille flow, which is linearly unstable with respect to two-dimensional disturbances at a Reynolds number of 5772.22, has a constrained absolute stability eigenvalue of 175.95, representing reduction by a factor comparable with the values above.

The six points connected with a solid smooth curve do all lie in the $R = R^* = 25000$ plane, but subsequent shifted curves connect points which do *not* all lie in the same $R = R^*$ plane. This procedure is appropriate to the degree that the results are asymptotic and independent, therefore, of R and R^*. As numerical results in this section illustrate, variations in the appearance of figures 4, 7, 9 and 10 at a higher R would be slight. We believe that the qualitative features are robust, but parallelism,

or slight departures therefrom, in adjacent curves should be interpreted as yet with caution. We hope to continue these studies with greater resolution of scale so that higher Reynolds numbers the degree to which these marginal curves do become asymptotic can be fully established. It is not impossible that some small logarithmic dependence on R remains; however it is below the level that we can deal with at present.

9. Conclusion

We conclude that, in a properly chosen Galilean frame, there is a time-independent mean flow, indistinguishable from the observed mean flow at arbitrarily large R, which is unstable to three-dimensional disturbances. It is also established that this flow is very close to the constrained absolute stability limit. It is most plausible then that both two-dimensional and three-dimensional linear instabilities play a central role in the physics of the statistically stationary turbulent field.

However the selective mechanisms (i.e. which A and K?) are not addressed here. They are not immediately visible in the graphical results. It may be that the simultaneous instability at many different scales of motion, found for the three-dimensional disturbances near the observed profile, is the determining feature. This path to turbulence would suggest a significant link with the more elementary dynamical systems whose connection with shear-flow turbulence has so far been more assertive than deductive. Although the empirical (A, K)-frame is inadequate for the exploration of marginality at all scales, it has simple integral properties which may provide guidance for further inquiry. One such property is the ratio of the fluctuation dissipation rate to the dissipation rate of the mean, uniquely determinable at each (A, K)-point. Figure 11 is a plot of this ratio, which exhibits extreme values on the marginal stability curves near the experimental values of (A, K). The properties of this extreme found from the general Euler–Lagrange model of the flow and (2.1) are being studied.

Present work suggests that a two-dimensional mean field can serve as a good first-order description of moments of the turbulent flow. In this paper, the solution of the equation for the full mean field has not been addressed. For that purpose, the Reynolds–Tiederman family of profiles has served as a substitute; however, consistent with a mean-field description, the fluctuation fields we have treated are governed by a linear Orr–Sommerfeld equation. Our sequence of numerical experiments with a freely chosen amplitude for the two-dimensional wave field show good agreement with observational data for reasonable wave amplitudes. Establishing this result as the solution of a complete two-dimensional mean-field problem is the first challenging problem emerging from this work. It is encouraging and intriguing that the energetic bound determined from the absolute stability of the smallest scale should also lie so close. It suggests a novel sense in which shear-flow turbulence manages to achieve that coalescene of absolute and marginal stability boundaries characteristic of the linear convection problem.

Solution of the mean-field problem will have both a rich spatial and temporal structure. Indeed, establishing contact with the detailed and more mechanistic studies of local bursts is an important goal. However, each facet of this new class of mean-field problems appears to be non-chaotic. Establishing in what sense a global description can capture the complex symbiotic relationship of two-dimensional and three-dimensional waves, which we believe governs the dynamics of bursts, is central in understanding both the limits of validity of a mean-field theory and the

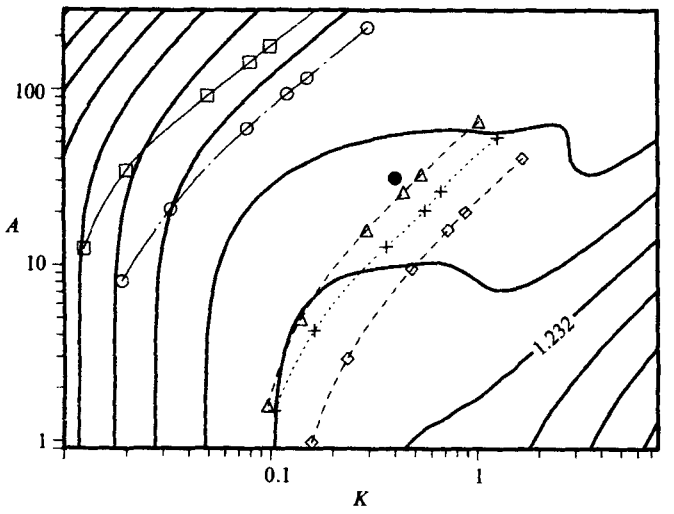

FIGURE 11. Contours of the logarithm of the ratio of fluctuation dissipation to mean dissipation at a profile Reynolds number of 25000. Note the occurrence of a maximum of this quantity along each of the neutral stability curves in the vicinity of the observed flow. The contour interval is 0.616, and the function increases to the right.

importance of fluctuation–fluctuation corrections. We are embarked on such study at this time.

Both authors received support for this work under Grant ATM81-18396 and the second author support also from Grant ATM84-08736 of the National Science Foundation, for which we are most grateful. Additionally we wish to thank Michigan Tech. for a generous allocation of computer time enabling us to undertake the three-dimensional eigenvalue calculations reported here.

REFERENCES

BUSSE, F. H. 1969. *Z. Agnew. Math. Phys.* **20**, 1.

BUSSE, F. H. 1978 *Adv. Appl. Mech.* **18**, 77.

CHAN, S. K. 1971 *Stud. Appl. Maths* **50**, 13.

CLAUSSEN, M 1983 *Boundary-Layer Met.* **27**, 209.

HERBERT, T. 1980 *AIAA J.* **18**, 243.

HERRING, J. 1963 *J. Atmos. Sci.* **20**, 325.

HERRING, J. 1964 *J. Atmos. Sci.* **21**, 277.

JOSEPH, D. D. 1976 *Stability of Fluid Motions. Springer.*

JOSEPH, D. D. & CARMI, S. 1969 *Q. Appl. Maths.* **26**, 575.

KRAICHNAN, R. H. 1962 *Phys. Fluids* **5**, 1374.

MALKUS, W. V. R. 1956 *J. Fluid Mech.* **1**, 521.

MALKUS, W. V. R. 1979 *J. Fluid. Mech.* **90**, 401.

MALKUS, W. V. R. & PROCTOR, M. R. E. 1975 *J. Fluid Mech.* **67**, 417.

ORSZAG, S. A. 1971 *J. Fluid Mech.* **50**, 689.

ORSZAG, S. A. & PATERA, A. T. 1981 *J. Fluid Mech.* **128**, 347.

REYNOLDS, W. C. & TIEDERMAN, W. G. 1967 *J. Fluid Mech.* **27**, 253.

ZAFF, D. 1987 Secondary instability in Ekman boundary flow. Ph.D. thesis, Department of Mathematics, Massachusetts Institute of Technology.